# On-Orbit Absolute Radiance Standard for Future IR Remote Sensing Instruments

Fred A. Best, Douglas P. Adler, Claire Pettersen, Henry E. Revercomb, P. Jonathan Gero, Joseph K. Taylor, Robert O. Knuteson
Space Science and Engineering Center
University of Wisconsin
Madison, WI, USA
fred.best@ssec.wisc.edu

John H. Perepezko
Materials Science and Engineering
University of Wisconsin
Madison, WI, USA

***Abstract*—Space borne IR remote sensing instruments in the future will require higher accuracies than now available, and the ability to perform absolute on-orbit calibrations traceable to SI standards. An On-Orbit Absolute Radiance Standard (OARS) is being developed to provide these on-orbit calibrations. The OARS uses a high emissivity (>0.999) blackbody cavity with imbedded thermistor temperature sensors that can be periodically calibrated using the transient melt signatures from three different reference materials also imbedded in the cavity. Emissivity measurements of the blackbody can be made periodically by measuring the reflection of a carefully baffled heated cylinder placed in front of the cavity.**

***Keywords- Remote Sensing IR Instrument Calibration***

## I. INTRODUCTION

Future NASA infrared remote sensing missions, including the climate benchmark CLARREO mission will require better absolute measurement accuracy than now available, and will most certainly rely on the emerging capability to fly SI traceable standards that provide irrefutable absolute measurement accuracy [1]. As an example, instrumentation designed to measure spectrally resolved infrared radiances with an absolute brightness temperature error of better than 0.1 K will require high-emissivity (>0.999) calibration blackbodies with emissivity uncertainty of better than 0.06% (k=3), and absolute temperature uncertainties of 0.045K (k=3). Key elements of an On-Orbit Absolute Radiance Standard (OARS) meeting these stringent requirements have been demonstrated in the laboratory at the University of Wisconsin and are undergoing further refinement under the NASA Instrument Incubator Program (IIP). This work will culminate with an integrated subsystem that can provide on-orbit end-to-end radiometric accuracy validation for infrared remote sensing instruments.

## II. APPROACH

Figure 1 illustrates the key features of the OARS in a section view. The blackbody design is based on the on-board calibration system developed for the NASA Geosynchronous Imaging Fourier Transform Spectrometer [2]. A temperature controlled light-trapping blackbody cavity (with a 30 mm aperture) contains thermistor temperature sensors and miniature phase change cells that provide on-orbit temperature calibration [3]. Three or more phase change cells with different reference materials can be used, thus providing multiple calibration temperatures. The heatable conical frustum (heated halo) out in front of the cavity provides the broadband source for periodic measurement of emissivity [4]. These measurements are made by the spectroradiometer that normally views the cavity for calibration verification, but in this case it is measuring the reflected signal of the heated halo. With the knowledge of the heated halo and effective background temperatures, and the solid angle view factor of the cavity view to the halo, the cavity emissivity can be calculated. Laboratory measurements of an OARS type blackbody, with a spectral emissivity greater than 0.999, have been made with uncertainties less than 0.0004 (k=3).

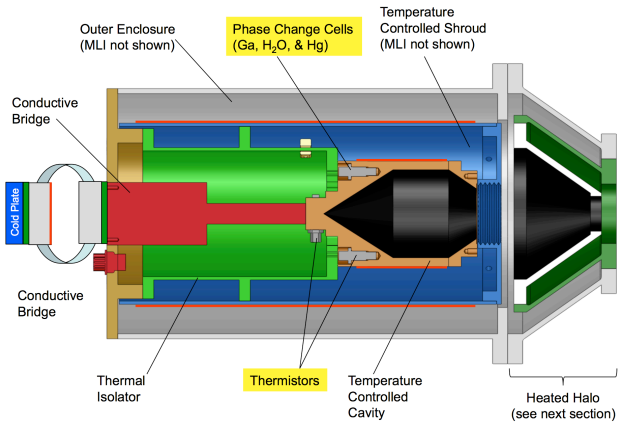


Figure 1. The key features of the OARS.

A temperature calibration point is obtained by measuring the transient cavity temperature response to a small increase in power. The sequence of events during a typical melt of gallium is illustrated in Figure 2. After initial stabilization in the constant temperature mode, a constant power is used to transition through the melt plateau, where the phase change signature is observed. Note that these signatures are clearly discernable even though there is less than 1 gram of melt material. Other melt materials have been demonstrated,

including $H_2O$, Hg, and a Ga-Sn eutectic. Using this technique, the thermistors imbedded in the cavity can be calibrated to uncertainties of better than 5 mK (k=3). With the inclusion of all other error sources, this leads to a total uncertainty of the OARS blackbody $T_{eff}$ of 45 mK (k=3).

The spectral radiance $I_{\tilde{\nu}}$ emitted by the OARS is

$$I_{\tilde{\nu}} = \varepsilon_{\tilde{\nu}} B_{\tilde{\nu}}(T_{eff}) + (1-\varepsilon_{\tilde{\nu}}) I_{\tilde{\nu},bg} \qquad (1)$$

where $T_{eff}$ is the effective temperature of the blackbody cavity, $\varepsilon_{\tilde{\nu}}$ is the cavity emissivity, and $I_{\tilde{\nu},bg}$ is the radiation from the background environment. The effective temperature is determined by a weighting of the different thermistors imbedded at key locations within the cavity. The weighting has been determined from analysis that uses a Monte-Carlo ray trace model of the cavity with a temperature distribution calculated from a thermal model.

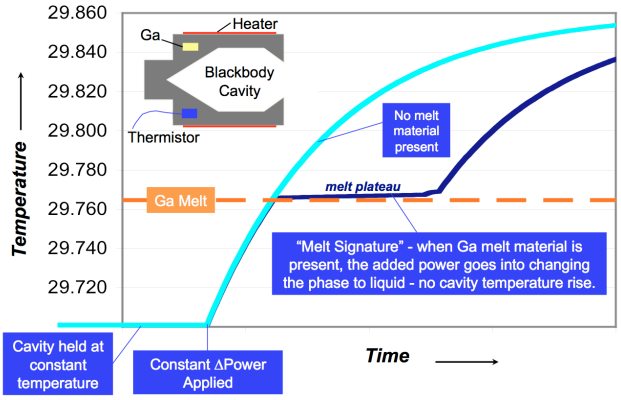


Figure 2. Key elements of a transient melt signature, in this case for Gallium. The melt plateau is approximately 4,000 seconds in duration.

## III. Experimental Results

### A. Phase Change Cells

The melt materials are individually confined into miniature welded phase change cells. After defining the detailed containment configuration, the phase change cells were subjected to a full accelerated life test that was designed to simulate the expected mission temperature soak and cycling environmental exposure. Tests were devised to show that the phase change materials have not been unacceptably contaminated via dissolution, and that the containment materials are not mechanically compromised via mechanisms such as liquid metal embrittlement. Mechanical integrity was also investigated by comparing the housing morphology both before and after the accelerated life testing. In addition, significant testing has been conducted to explore the melt plateau repeatability, and to characterize the relationship between the time taken to go through the melt and the melt plateau (mid-melt) temperature.

Fig. 3 illustrates that as the time to go through the melt is increased, the mid-melt temperature asymptotically approaches the known (in this case) gallium melt temperature. This characteristic asymptotic behavior has shown to be invariant for a given physical configuration. This is the case for all three melt materials. The inset plot on the upper right of Fig. 3 illustrates the excellent melt plateau repeatability for three different runs taken before and after exposure to accelerated life testing.

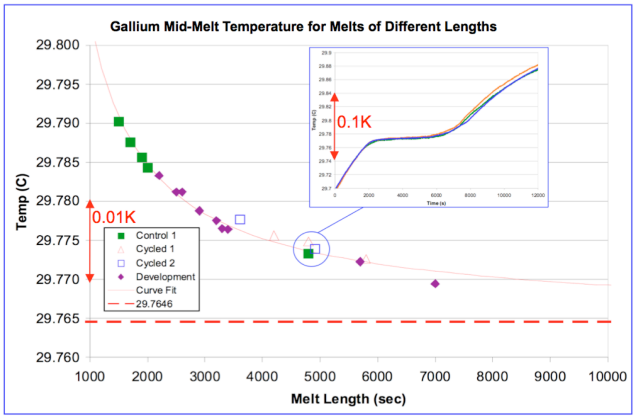


Figure 3. The inset plot at upper right shows the three melt signatures associated with the circled data points. Data included in the plot is from three different phase change cells taken before and after a full duration hot soak and deep temperature cycling.

The definitive test of the melt cell performance is the melt signature. All three melt materials, gallium, water, and mercury have undergone extensive examination of the melt signature behavior in several different configurations as well as before and after a full accelerated life test, with excellent agreement [3]. As seen in Fig. 4, the signatures for all three melt materials fall within about ±2mk of the characteristic mid-melt temperature versus melt length curve, regardless of orientation, pre or post life test, or housing to housing variation.

### B. Heated Halo

The spectral radiance $I_{\tilde{\nu}}$ emitted by a cavity with a finite aperture with Lambertian reflectance is given in Eq. (1). The dominant source of uncertainty in a well designed blackbody arises from the measurement of the cavity temperature and the effect of the nonunity emissivity of a practical blackbody with a macroscopic aperture. In this section we address the on-orbit monitoring of blackbody cavity emissivity using the Heated Halo.

The Heated Halo is a broadband thermal radiation source designed to fill a large fraction of the solid angle of a given blackbody's field of view, while being physically outside of the field of view of the detector observing the blackbody. The Heated Halo used in this experiment is a hollow aluminum cylinder, painted black and heated with Kapton thermofoil heaters to 95°C (Fig. 5).

For this experiment, we measured the emissivity of the Atmospheric Emitted Radiance Interferometer (AERI) blackbody [5]. The blackbody employs a light-trapping cavity geometry, is painted with diffuse Aeroglaze Z306, and its temperature is measured by embedded thermistors to within a combined uncertainty of 0.05 K ($k$=3). The blackbody is operated at ambient room temperature (about 23°C).

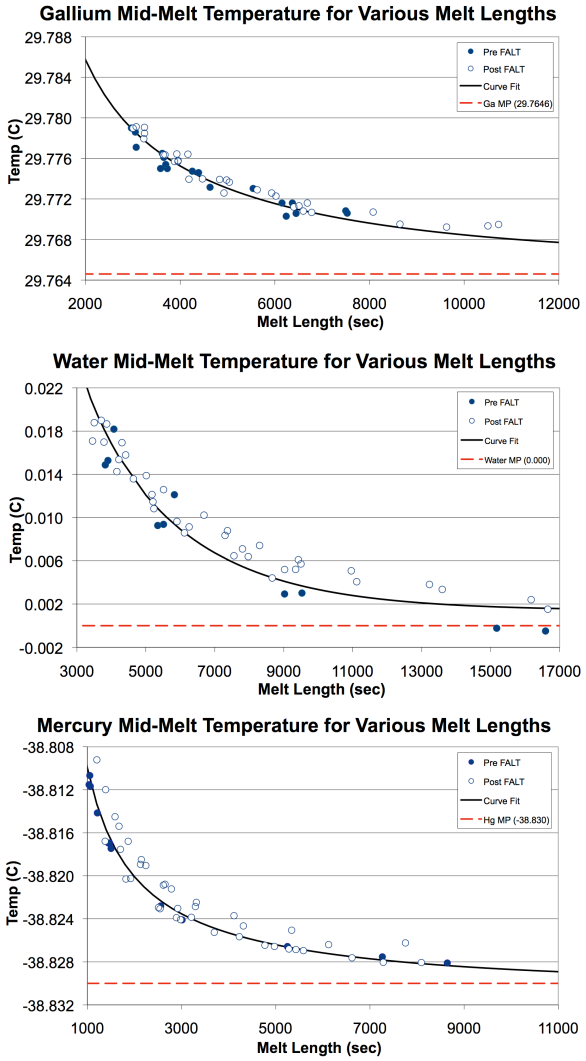


Figure 4. Plots of the characteristic curves for the gallium, water, and mercury melt housing samples.

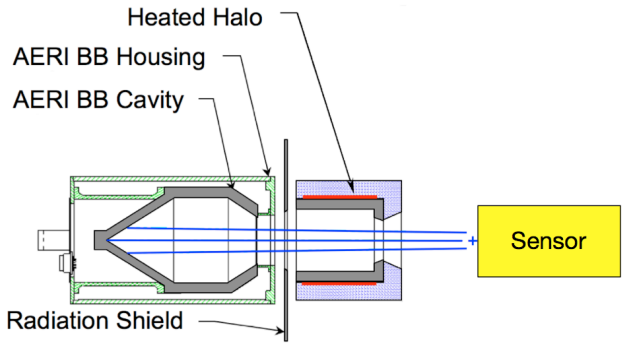


Figure 5. Schematic cross-sectional representation of the first generation Heated Halo. A radiation shield reduces radiative heating of the blackbody by the Heated Halo.

Two different spectrometer systems were used to observe the AERI blackbody: (1) the Scanning High-resolution Interferometer Sounder (S-HIS), a Fourier transform spectrometer (FTS) designed for autonomous operation on board research aircraft, covering the 580-2800 $cm^{-1}$ spectral range using an InSb and two HgCdTe detectors [6]; and (2) the Absolute Radiance Interferometer (ARI), a laboratory-based FTS covering the 200-1700 $cm^{-1}$ spectral range using a pyroelectric detector [7].

When the Heated Halo is placed in the optical chain between the spectrometer and the blackbody, the background radiance in Eq. (1) becomes,

$$I_{\tilde{\nu},\mathrm{bg}} = FB_{\tilde{\nu}}(T_{\mathrm{ha}}) + (1-F)B_{\tilde{\nu}}(T_{\mathrm{rm}}^{\mathrm{eff}}) \qquad (2)$$

where $F$ is the geometrical view factor characterizing the fraction of the blackbody solid angle viewing the Heated Halo, $T_{\mathrm{ha}}$ is the Heated Halo temperature, and $T_{\mathrm{rm}}^{\mathrm{eff}}$ is the effective temperature of the background environment. Eq. (1) can be rewritten as

$$\varepsilon_{\tilde{\nu}} = (I_{\tilde{\nu}} - I_{\tilde{\nu},\mathrm{bg}}) / (B(T) - I_{\tilde{\nu},\mathrm{bg}}) \qquad (3)$$

where $I_{\tilde{\nu},\mathrm{bg}}$ is given by Eq. (2). All of the terms on the right hand side of Eq. 3 can be measured or modeled accurately, thus the spectral emissivity for a given blackbody can be evaluated.

The emissivity spectrum of the AERI blackbody, measured by both the S-HIS and the ARI using the Heated Halo method, is shown in Fig. 6, compared to a model result from a Monte Carlo simulation [8]. The overall shape of the observed emissivity curve, notably the step in emissivity around 1200 $cm^{-1}$, is consistent with the properties of the Aeroglaze Z306 paint [9]. Some of the high frequency oscillations in the measurements can be attributed to detector noise (type A uncertainty), as well as spectral lines of carbon dioxide (near 667 $cm^{-1}$) not fully eliminated by the purge employed in the experiment. The lower measured values in emissivity between 600-1000 $cm^{-1}$, compared to the model result, indicate an error in the model parameterization due to extrapolation.

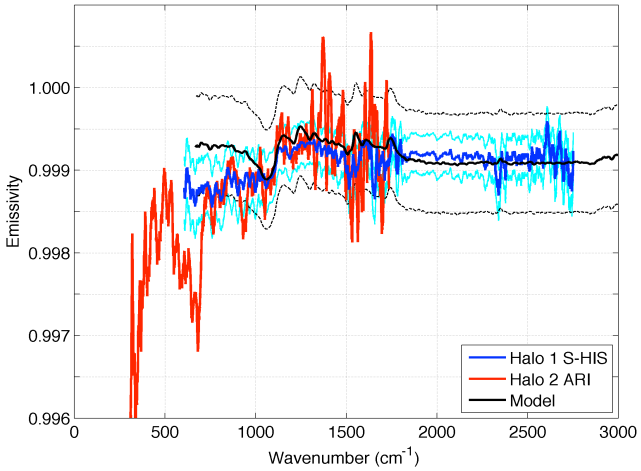


Figure 6. Comparison between two versions of Heated Halo measurements, S-HIS (blue) and ARI (red), as well as the modelled emissivity of the AERI blackbody. The dashed curves represent the systematic (type B) uncertainty (k=3) for the S-HIS and the model result.

The six main sources of systematic measurement uncertainty (type B: stray radiation, view factor, calibration accuracy, Heated Halo temperature, effective room

temperature, blackbody temperature) are calculated by applying variational analysis to Eq. 4. The overall root-sum-of-squares (RSS) uncertainty is less than $4\times10^{-4}$ ($k$=3) between 500-2800 $cm^{-1}$, and has a maximum value of $1.2\times10^{-3}$ ($k$=3) at 200 $cm^{-1}$.

In summary, using the S-HIS and ARI spectrometers, the spectral emissivity of the AERI blackbody was measured in the 200-2800 $cm^{-1}$ spectral range with the Heated Halo method. The measurements are in agreement with each other, as well as with a Monte Carlo model, within their uncertainties. Furthermore they are in agreement with several other measurements of the AERI blackbody emissivity using physically independent methods in experiments performed by NIST. The low level of systematic (type B) experimental uncertainty across most of the infrared spectrum ($4\times10^{-4}$, $k$=3) is encouraging that the Heated Halo can be deployed on space-based instruments to monitor calibration blackbody emissivity, on-orbit, throughout the lifetime of satellite missions.

The final packaging and configuration for the heated halo is the conical frustum shape shown in OARS diagram (Fig. 1). This geometry (especially the view factor of the cavity to the halo) is very similar to the test configurations described above, except an enhanced black paint will be used in the cavity to increase the emissivity out to 50 µm. The OARS is expected to be completed soon and ready for testing with the ARI spectrometer.

## IV. Microgravity Demonstration on the ISS

NASA has provided a separate grant, under PI Martin Mlynczak of LaRC, to demonstrate the performance of the UW melt cell concept on the International Space Station, sometime within the next year. The configuration planned for this demonstration is shown in Fig. 7. The phase change cells are contained in the aluminum melt block, along with the temperature sensor to be calibrated. The aluminum shield cap is thermally coupled to the top Thermo Electric Cooler (TEC) plate. Two TECs are sandwiched between the melt block and a heat sink, which the TECs use to draw/reject heat in order to heat and cool the melt block. The bottom TEC provides a level of isolation from ambient temperature fluctuations, which allows the top TEC to maintain greater stability. The outer case is held at constant temperature using a heater to provide a stable environment. The temperature control and data collection for this demonstration are provided by the Experiment Support Package developed by Utah State Space Dynamics Laboratory. Because the Experiment Support Package does not have the capability to get to the freezing point mercury, we plan to use a binary eutectic of gallium as our third material along with gallium and water.

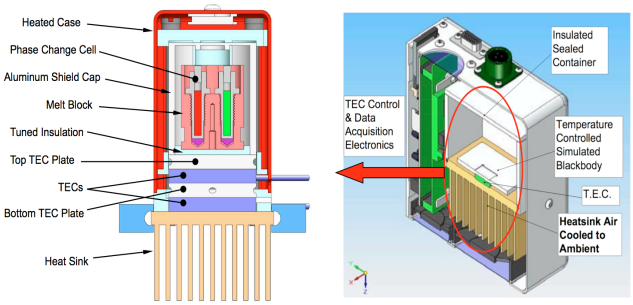


Figure 7. The configuration for microgravity demonstration of the phase change includes three different melt materials and makes use of the Experiment Support Package developed by Utah State Space Dynamics Laboratory.

## V. Conclusions

Key aspects of an on-orbit absolute radiance standard, capable of periodic self-calibration traceable to SI standards, have been demonstrated in the laboratory, to accuracies required for future IR remote sensing instruments, including CLARREO. Temperature calibration is conducted using melt signatures of miniature phase change cells. Emissivity of the blackbody is measured by the spectroradiometer that views the reflected signal from a heated halo that is located in front of the cavity.

## Acknowledgment

The technology advancement phase of this work is being conducted under NASA IIP grant NNX08AN35G. The microgravity demonstration is being conducted under NASA grant NNX09AK45G.

## References

[1] National Research Council, Earth Science and Applications from Space: National Imperatives for the Next Decade and Beyond, National Academies Press, Washington D. C., (2007).

[2] F. A. Best, H. E. Revercomb, D. C. Tobin, et al.; Performance verification of the Geosynchronous Imaging Fourier Transform Spectrometer (GIFTS) on-board blackbody calibration system. Proceedings of SPIE Vol. 6405, 64050I (2006).

[3] F. A. Best, D. P. Adler, C. Pettersen, et al.; On-orbit absolute temperature calibration using multiple phase change materials: overview of recent technology advancements. Proceedings of SPIE Vol. 7857, 78570J (2010).

[4] P. J. Gero, J. K. Taylor, F. A. Best, et al.; On-orbit absolute blackbody emissivity determination using the heated halo method. Proceedings of SPIE Vol. 7857, 78570L (2010).

[5] R. O. Knuteson and Coauthors, Atmospheric Emitted Radiance Interferometer. Part I: Instrument Design, J. Atmos. Oceanic Technol., 21, 1763–1776, 2004.

[6] H. E. Revercomb and Coauthors, Highly accurate FTIR observations from the scanning HIS aircraft instrument, in Proc. SPIE 5655, 41–53, 2005.

[7] J. K. Taylor and Coauthors, The University of Wisconsin Space Science and Engineering Center Absolute Radiance Interferometer (ARI), in Proc. SPIE 7857, 78570K, 2010.

[8] F. A. Best and Coauthors, Determination of the Atmospheric Emitted Radiance Interferometer (AERI) blackbody emissivity and radiance using multiple techniques, in Proc. Characterization and Radiometric Calibration for Remote Sensing, Logan, UT, 2009.

[9] M. J. Persky, Review of black surfaces for space-borne infrared systems, Rev. Sci. Instrum., 70, 2193–2217, 1999.